Hybrid RANS-LES Modelling of Flows with Large Separated Regions

Stefan Leicher EADS-MAS, Germany

Summary

It is well known that the unsteady contents of flows with massive detached boundary layers, large embedded separated regions and unstable vortices can not always be adequately modelled by common RANS/URANS methods. Within the 7th EC Framework Research Project DESIDER the usefulness of LES- and hybrid RANS/LES- (DES Spalart et al. 1997, DDES Spalart et al. 2006) methods for such flow phenomena was proven. To answer questions for unsteady pressure and aero-acoustic loads upon structures and noise production the latter are increasingly introduced in routine work within industry, mainly because of their acceptable balance between accuracy of the results and computational effort.

This paper will demonstrate the worth of such hybrid methods for two test cases. The generic FA5 aircraft configuration at high angle of attack including various interacting vortex systems, exhibiting separation, vortex breakdown and buffeting phenomena on wings and severe vortex interaction and buffeting of the vertical tail plane. The simulations at subsonic speed will be compared with experiments by means of mean flow properties, time dependent fluctuations and their spectral content. The second configuration will be the rectangular M219 cavity (Stanek et al. 2000) at M_∞ = 0.85 and 1.35. This case is dominated by unsteadiness forced by separated boundary layers, unstable shear layers and moving vortices. Here the main interest is taken into the prediction of the unsteady pressure oscillations inside the cavity and the well known aero-acoustic resonance separation and their spectral distribution. Both test cases were part of the EC-DESIDER project (Haase et al., 2009).

1 Cavity

In aeronautic applications, typical cavity flows can be observed over, for example, a landing-gear housing well and weapon-bays, which are often characterized by unsteadiness, boundary-layer detachment and separation, as well as by shear-layer instabilities and vortex motions. Since the pioneering work of Roshko (1955), cavity flows have been extensively studied by means of theoretical and numerical analysis (Peng 2008) and by experimental measurements. Due to inherent pressure oscillations, a cavity flow is usually prone to aero-acoustic resonance, which can cause structural damage or intolerable accelerations of electronic equipment or even instability of the total aircraft The simulated M219 cavity is of the open type, whose acoustic tones are generated by the interaction between the shear layer, which covers the cavity opening, and the cavity aft wall on which it impinges. Corresponding to the characteristic pressure patterns (standing waves and modes) in the cavity, the frequencies of acoustic tones can be approximately determined by an empirical formula due to Rossiter (1964), viz.

$$f_n = \frac{U_\infty}{L} \frac{n-\gamma}{M_\infty + 1/\kappa}, \tag{1}$$

where U_∞ and M_∞ are, respectively, free stream velocity and Mach number, L is the cavity length, n is the mode number, γ and κ are two empirical constants.

In this presentation the modelling of a turbulent cavity flow using the Detached Eddy Simulation (DES, Spalart et al., 1997) and the X-LES model (Kok et al., 2004) for two different Mach numbers will be shown. The main focus will be given to the calculated pressure distribution along the bottom of the cavity and the detected distinct acoustic tonal modes in comparison with available experimental data (Stanek et al., 2000). Furthermore some instantaneous flow features will also be presented

1.1 Simulation and Results

The flow around a rectangular generic cavity with an aspect ratio of $L:D:W = 5:1:1$ is simulated for Mach number M = 0.85 using the SA-DES and the X-LES model and for 1.35 using the SA-DES model only. The cavity is placed in a on a flat surface in a wind tunnel. The unstructured grid contains about 6.18 million nodes with a prismatic elements patched over the wall surface. Figure 1 illustrates the computational grid and the cavity sketch. As in the experimental setup (Stanek et al., 2000), the cavity is embedded in a flat plate held by a sting.

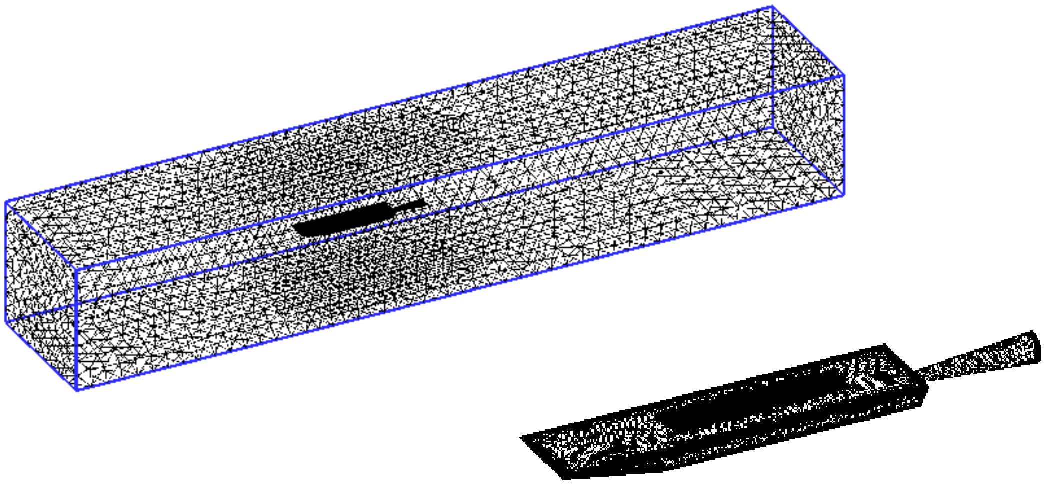

Figure 1: Computational grid

The TAU (Schwamborn at al. 2006) code has been used to perform the computations.

The cavity flow is suitable for DES modelling for the fact that the upcoming thin boundary layer is “detached” from the leading edge of the cavity. The detached flow is subsequently contained by the cavity, being characterized by the instability of the mixing layer over the cavity opening and by unsteady vortex motions inside the cavity. The unsteadiness is due to self-sustained oscillations caused by the impact of the shear layer on the cavity rear wall. While the near wall boundary layer is treated in RANS mode the mixing layer and the off-wall vortex motions in the cavity are modelled by the LES mode.
In the experiment conducted by QinetiQ (Stanek et al., 2000), the pressure fluctuations were measured on the cavity floor surface at ten locations along the stream wise *x*-direction (being denoted respectively k20-k29), which were distributed uniformly over a range of *x/L* = 0.05–0.95 (*x/L* = 0 is set at the cavity leading edge).
In the computation, along with the statistic time-averaging analysis after the resolved flow being fully developed, the surface pressure at these measured locations has been monitored at each time step of 0.0002 seconds. The total sampling time period is about 0.5 seconds for all calculations.

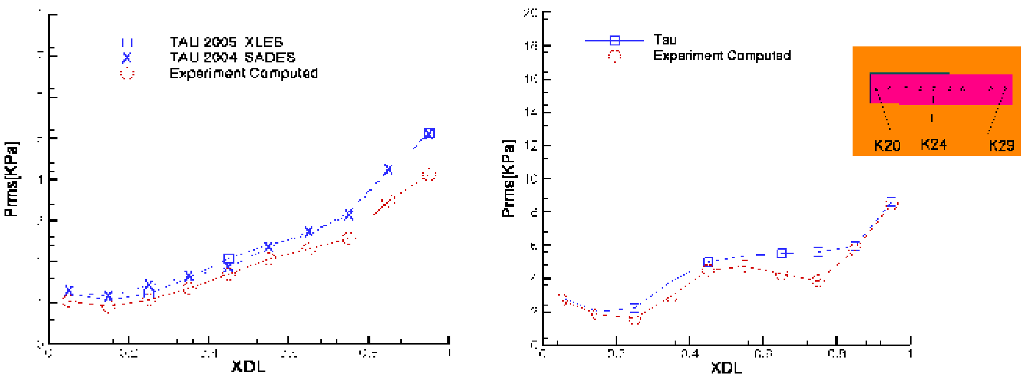

Figure 2: Overall RMS-distribution of pressure along bottom $M_\infty = 0.85$ (right) and $M_\infty = 1.35$ (left)

Both computations show a comparable good agreement with the experiment. For the lower Mach number SA-DES and X-LES show similar results with the SA-DES giving slightly better agreement in the centre part. A deviation from the tendency of the experimental curve starting at the middle of the cavity can be detected at both Mach numbers. Note the much higher RMS level with $M_\infty = 1.35$.
The spectral analysis of the RMS-distribution is shown in next figure for the most forward and backward pressure tube (K20 and K29). The agreement with the empirical formulation of Rossiter for the distinct peaks, representing the tonal modes, is quite good although the amplitudes are somewhat excessive, especially for the SA-DES simulation. The X-LES model seems to shift the peaks to slightly higher frequencies.

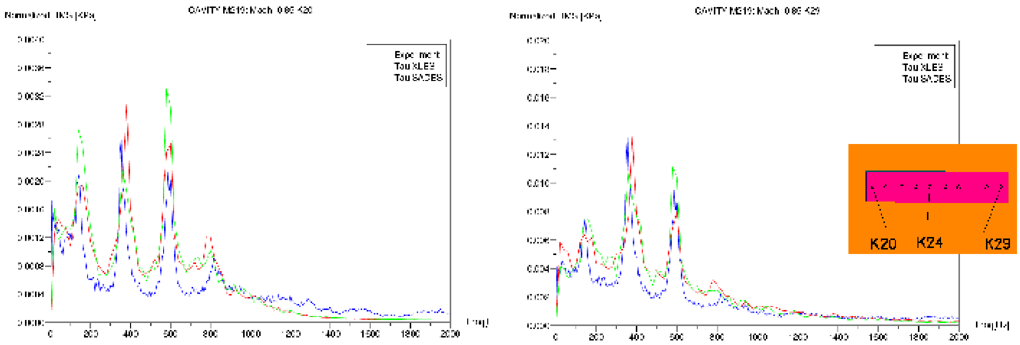

Rossiter frequencies (Eqn. 1): 148, 357, 566, 775 Hz

Figure 3 Spectral RMS-distribution of Pressure along bottom $M_\infty = 0.85$

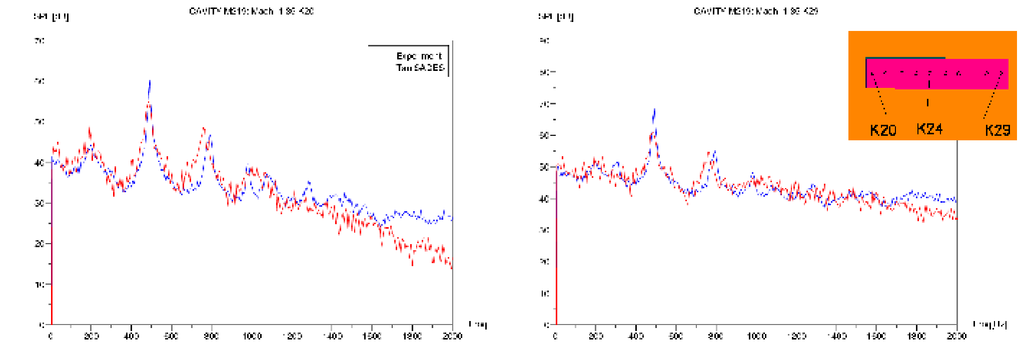

Rossiter frequencies (Eqn. 1): 198, 487, 765, 1013 Hz

Figure 4: Spectral RMS-distribution of pressure along bottom $M_\infty = 1.35$

For the higher Mach number distribution the sound pressure level (SPL) is calculated from the monitored pressure fluctuations by means of the power spectral density (PSD) using the following equation.

$$SPL = 20\log\left(\frac{\sqrt{PSD}}{2\times 10^{-5}}\right) \tag{2}$$

Again the simulation matches quite well the experimental results with regard to the location of the dominant frequencies with the peak amplitudes showing now better agreement. The discrepancy at the high frequencies can be attributed to the unresolved high fluctuation by the time step size of 0.0002 seconds and an inherent artificial dissipation in the models.

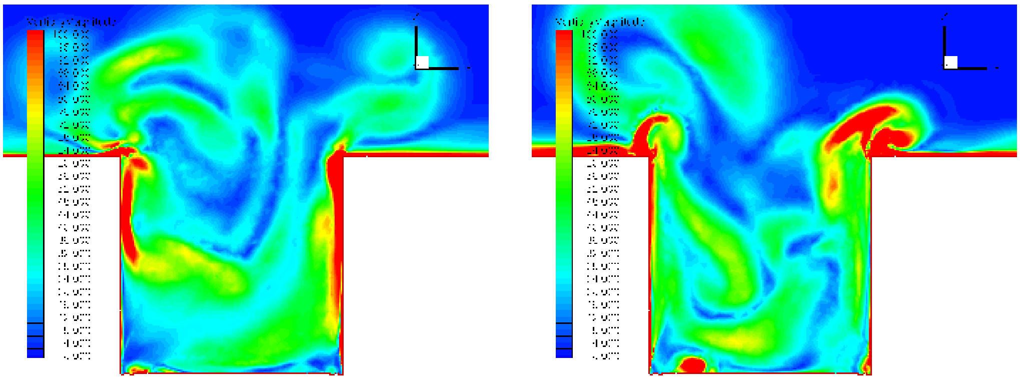

Figure 5: Instantaneous Vorticity distribution close to the Backward wall M = 0.85 and SA-DES (left) and X-LES (right).

The next two figures present instantaneous vorticity distributions comparing the SA-DES with the X-LES result. Similar features are resolved by both methods. Both models allow the resolution of rich large scale vortex motions. The shear layer emerging from the cavity opening sinks into the box and impinges the rear wall. The instability of the layer is clearly visible. Along the side wall the flow is ejected.

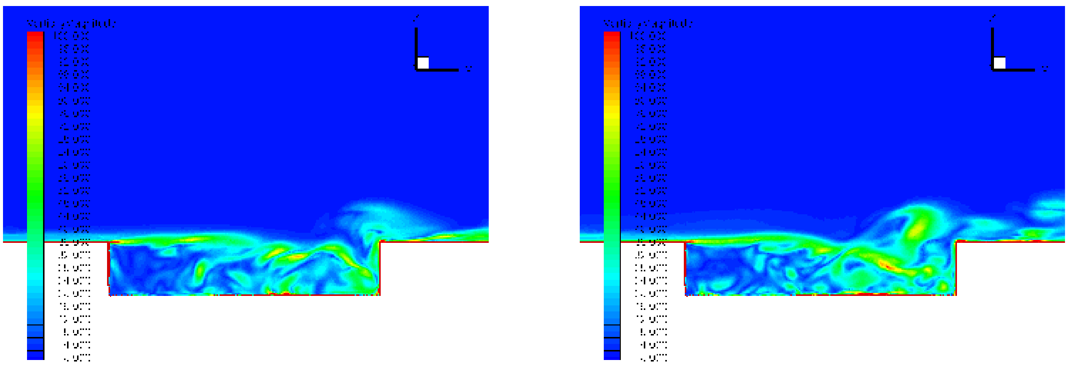

Figure 6: Instantaneous Vorticity distribution in the symmetry plane $M_\infty = 0.85$ and SA-DES (left) and X-LES (right)

Both hybrid models produce satisfactory agreement of the unsteady pressure patterns and the mean flow features. The predicted overall RMS pressure levels along the bottom of the cavity show good agreement with the experimental results although same differences in the tendency at the rear half can be observed. The spectral distributions as well as the distinct tonal peaks are simulated quite well giving good agreement with the empirical formula of Rossiter. There are some differences in the height of the amplitudes and at higher frequencies, the latter due to the relatively large time step size.

2. Generic Airplane

While the flow physics of generic delta wings with sharp leading edges are largely understood, complex realistic configurations with round leading edges, canards etc. are still of scientific and industrial interest.
This industrial example addresses the flow around a fighter type aircraft whose behaviour at high angle of attack is dominated by vortices. The industrial goals are the computational efficiency and a reasonable exact prediction of the force coefficients and the relevant frequencies of their unsteady content in the range of manoeuvres as well as the structural interaction.
The problem is to model the unsteady turbulent phenomena of vortex dominated flows at high angle of attack. It turned out from former computations in structured grids that URANS simulations give an insufficient description of the unsteady scales. Consequently a resolution of large scale flow fluctuations is necessary which can be better achieved by applying detached eddy simulations (DES Spalart 1997/2006). One hopes that DES modelling provides a better description of the vortex structure, and allows the identification of vortex burst and the identification and modelling of local unsteady effects in the flow field.
The flow conditions for this test case are a Mach number of 0.125, angle of attack of 15.0° and a Reynolds number of 2.8×10^6.
The flow around the generic FA5 fighter type configuration at 15° angle of attack and high Reynolds number has also been a DESIDER test case (Haase at al., 2009). The differences between the TAU code using the SA-DES (EADS) and SA-DDES (DLR, Lüdeke 2008) and the CFX SST-SAS (ANSYS 2007, Menter et al. 2005a/2005b) raised the question about the influence of the time step size which varies from 5.0×10^{-4} (DES) over 1.0×10^{-4} (DDES) to 5.0×10^{-5} (SST-SAS) seconds. Therefore the main focus of the current presentation will be the influence of the time step size on the DES and DDES model and a detailed comparison of these hybrid RANS-LES simulations with the experimental wind tunnel results.

2.1 Experimental Setup and Data

The experiments were performed by the TU Munich (Breitsamter 1997) in a wind tunnel with an open test with the measurements conducted with the X-wire technique. The main geometric features and a picture of the model in the wind tunnel are shown in figure 7.

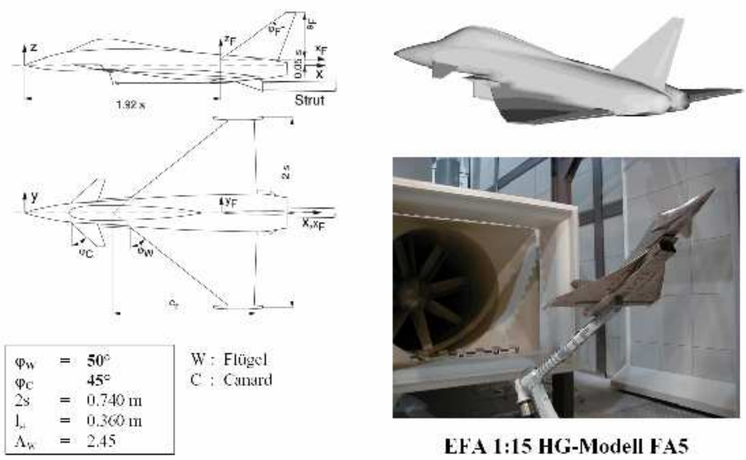

Figure 7: Wind tunnel model and experimental setup

Available experimental data comprise of mean velocity components, velocity RMS values, Reynolds stresses, vorticity magnitude and turbulent kinetic energy in twelve cuts. For each cut a matrix of about 31x25 values are given with a spacing of 1.4 cm in both directions.

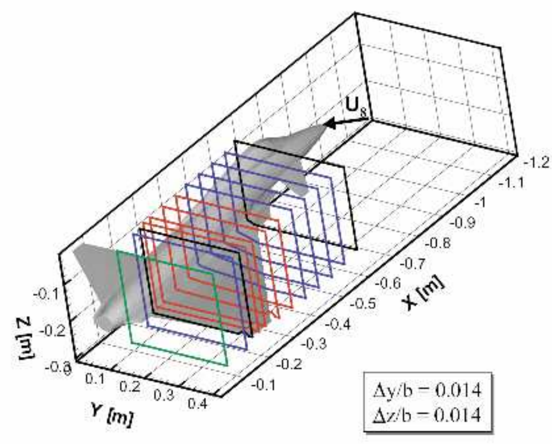

x/c_r	Punkte (Y x Z)
0.20	33 x 25
0.30	32 x 25
0.40	32 x 25
0.50	32 x 25
0.60	32 x 25
0.70	31 x 25
0.80	31 x 25
0.90	31 x 25
0.95	31 x 25
1.00	30 x 24
1.05	30 x 26
1.20	29 x 26

Figure 8: Location of the experimental data planes

2.2 Simulation and Results

The calculations are performed using an unstructured hybrid grid with about 13 million nodes. Grid details are shown in figure 9.

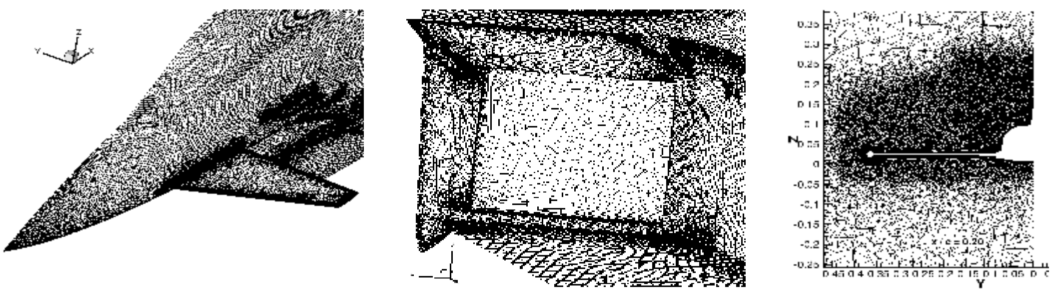

Figure 9: Grid details

The computations are performed using the TAU-code (Schwamborn 2006). Applied are the basic SA-DES and SA-DDES turbulence models, based on the so-called DES97 (Spalart at al. 1997) and Delayed DES model (Spalart at al. 2006).
The original time step size used from EADS within the DESIDER project (Haase at al. 2009) has been 5.0E^{-4} seconds and the data was monitored for about 1 second to collect statistic data. The results generated raised the question weather the differences between DES, DDES and SST-SAS can be attributed to the turbulence models or to the time step size.
Therefore a continuous reduction of the time spacing was applied to the DES and DDES model and the influence upon the comparison with the experiments of the TU Munich will be given below.
Special attention was paid to the mean u-velocity field because in all former calculations (Rieger 2005, Gurr 2006, Lüdeke 2008, Haase at al. 2009) using the structured as well as unstructured grids the level inside the vortex core turned become negative very early which could not be observed in experiment. The following sequence of figures show the development of the mean u-velocity for several x-stations.

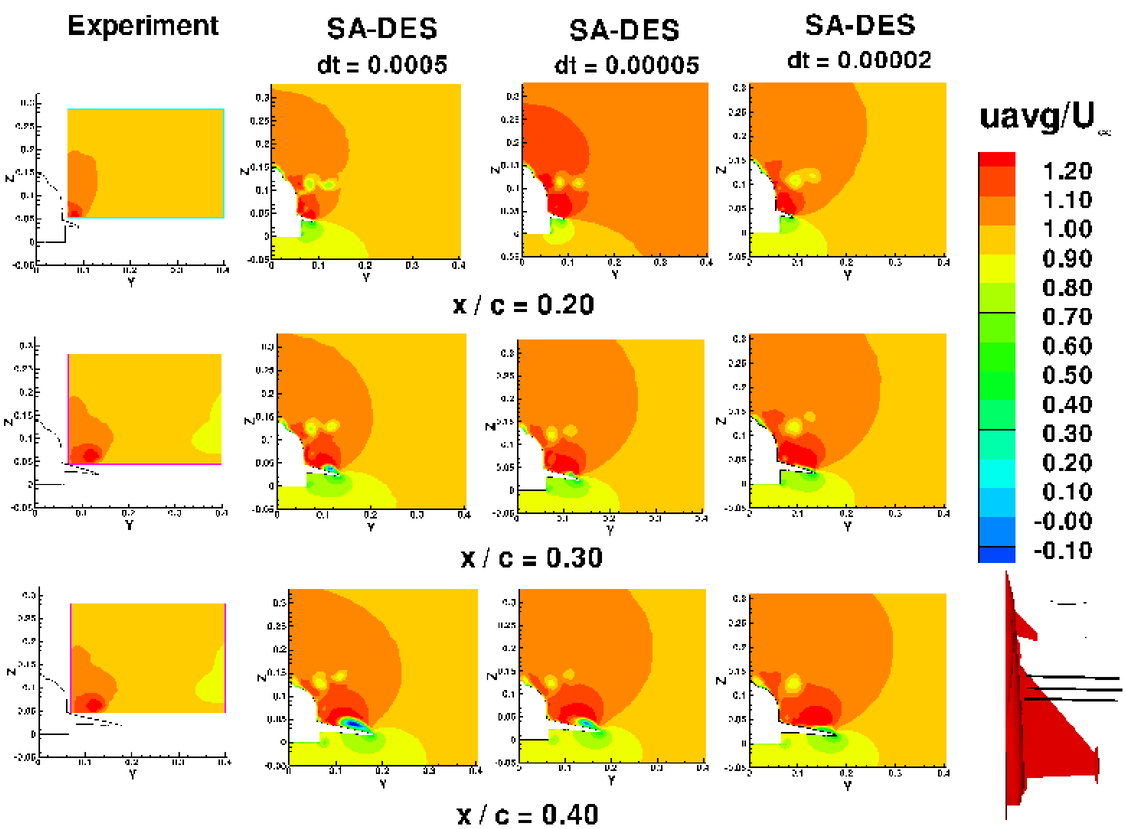

Figure 10: Comparison of mean u-velocity in cuts x/C=0.2, 0.3, and 0.4 for different time step sizes

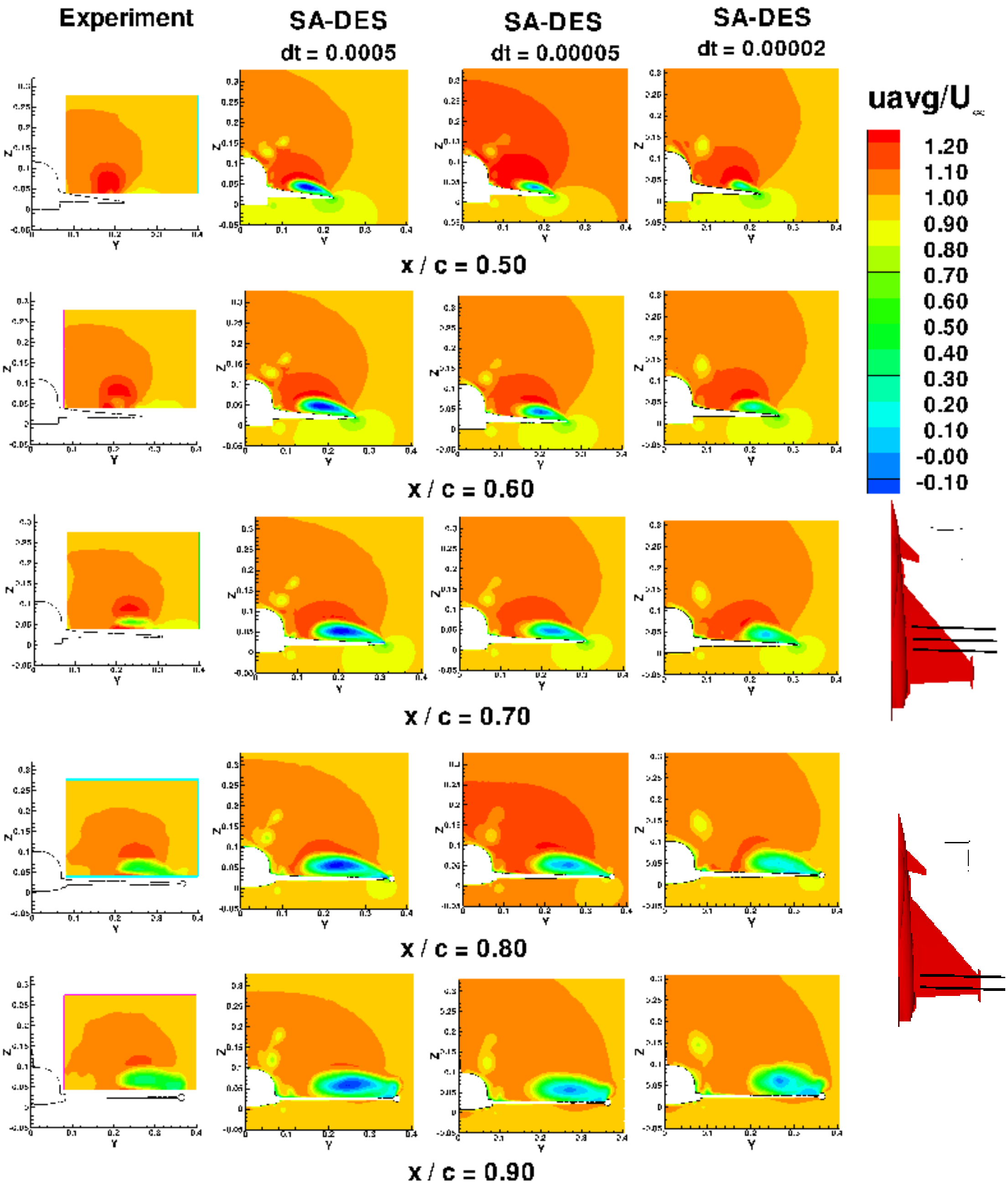

Figure 11: Comparison of mean u-velocity in cuts x/C=0.5, 0.6, 0.7, 0.8 and 0.9 for different time step sizes

The sequence of figures above show very clear the great influence of the time step size upon the mean axial velocity. With decreasing size the region and level of negative values is reduced and the comparison with the experiment improved. Remarkable seems to be the obvious further influence between $\Delta t=5x10^{-5}$ and $2x10^{-5}$ representing a factor 2.5 although it is not as great as for the first step (factor of 10). In the experiment the vortex break down – indicated by the lowest u-value – was found at x/C close to 0.6. For the original time step 2.0x10-4 the u-value turns to negative between x/C = 0.3 and 0.4. For the next smaller value of $5x10^{-5}$ this happens between 0.5 and 0.6 while for $2x10^{-5}$ the value keeps positive till x/C=0.90 with a local minimum between x/C 0.6 and 0.7. The influence is remarkable although the minimum level is still to low. Also the shape corresponds much better with the experimental distribution because the extension in span is reduced. For all time step sizes one can observe an over prediction of the canard vortex at all x/C stations which is not visible in the experiments shown in the first column. The time step sequence shows something like an asymptotic behaviour with regard to the differences. The still missing gap compared to the experiment may be due to an insufficient resolution of small turbulent structures in this region probably caused by a still too coarse grid.

For the cut x/C=0.80 once more the continuous reduction of the negative u-mean region is shown. Also marked are the locations from three of the field points (as white dots), where the flow properties are monitored for later spectral analysis. The figure presents further that also the level and distribution of the other components are improved as well. The size of the negative v-velocity continuously reduces and the location of the negative w-component above the wing is step by step shifted more outboard, both effects improve the agreement with the measurements.

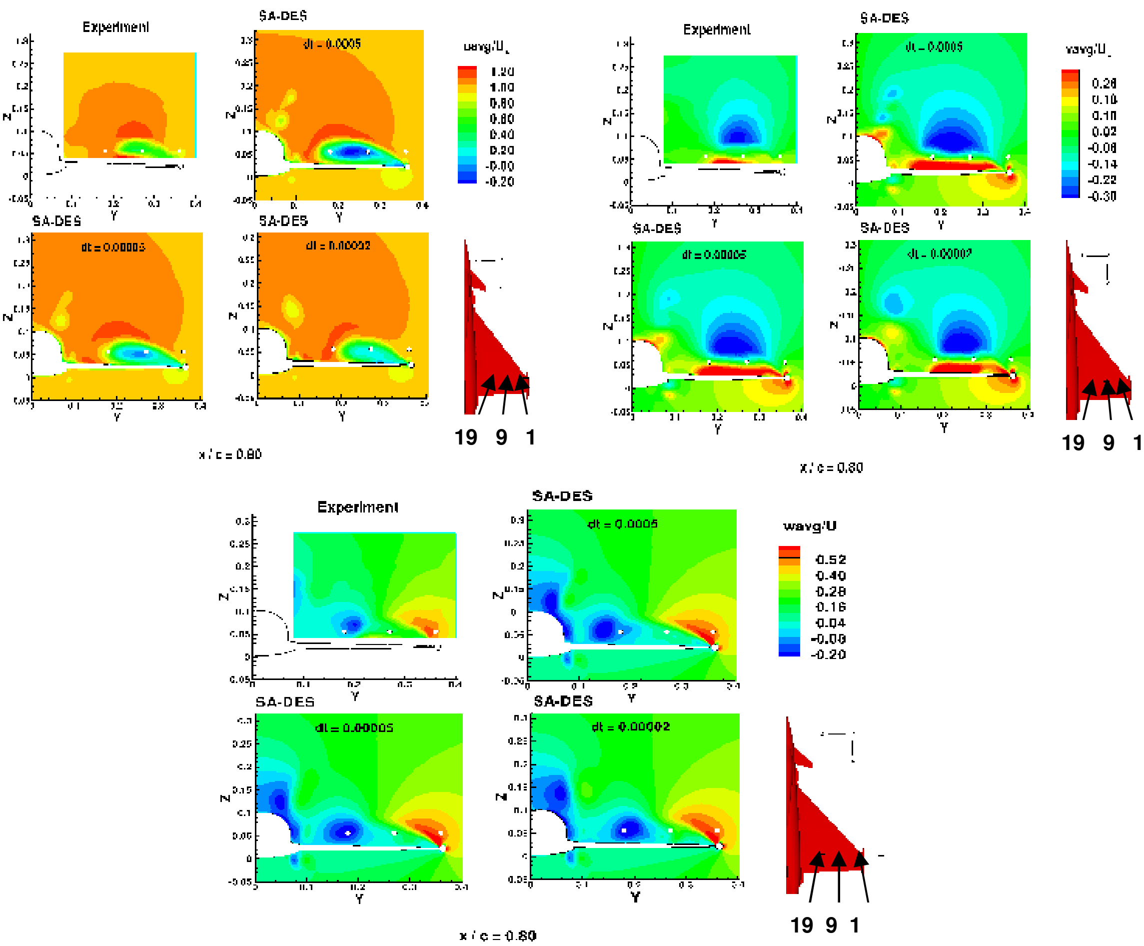

Figure 12: Comparison of mean velocities in cut x/C= 0.8 for different time step sizes with positions of monitored flow properties

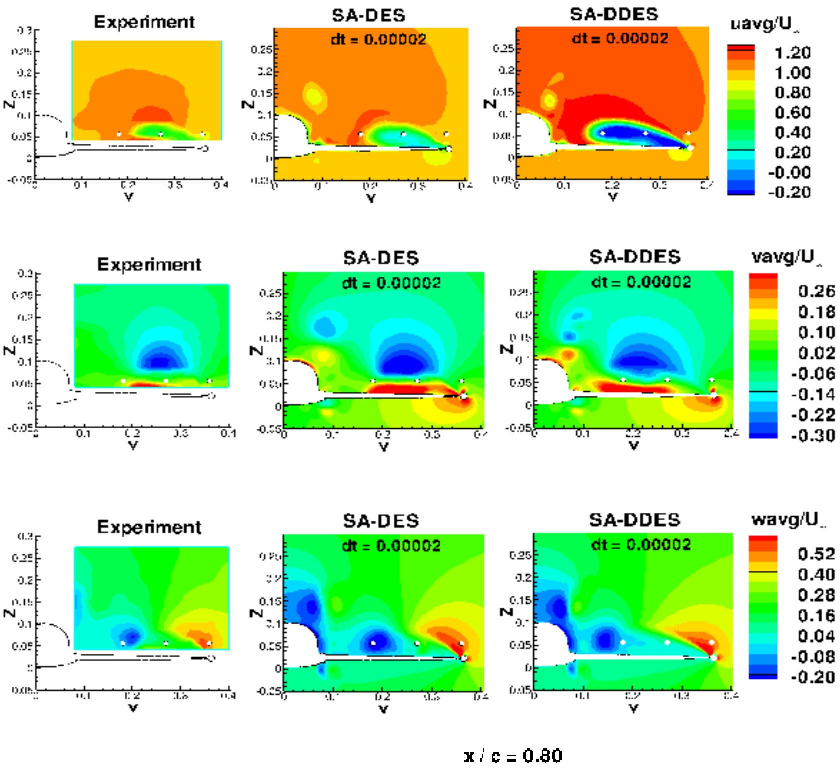

Figure 13: Comparison of the influence of the time step between DES and DDES on mean velocities in cut x/C = 0.8

Astonishing is that the time step reduction for the DDES model has not a comparable influence upon the level and distribution as for DES. This effect is at the moment not understood at needs further investigations.
Important for the unsteady content of the flow and its impact upon the structure are the local fluctuations of the properties. The time output for the velocity components and a spectral analysis will be shown for the three points 1, 9 and 19 as already indicated. These points are located near the trailing edge at x/C=0.8 and somewhat above the wing surface. Point 1 is the most outboard while 19 is the most inboard location. As can be conclude from the figure above the values of point 19 might be most sensitive because it is positioned right at the boundary between vortex and "free flow". Depending on the size of the vortex core the point is situated outside (experiment and DES $\Delta t=2x10^{-5}$), close to the border (DES $\Delta t=5x10^{-5}$ and DDES $\Delta t=2x01^{-5}$) or inside the vortex ($\Delta t=5x10^{-4}$).

The time history and a spectral analysis of the velocity components are given below. As expected point 19, which is located most inboard, shows the largest deviations. Looking at the time histories as well as at power spectral density distribution one can conclude that theory shows larger amplitudes for all three velocity components in all three points monitored. For the u-component the refined time step results are very close together. The mean value at point 1 is more or less in the middle between the old result and the experiment. For point 9 in the middle of the vortex the mean value changes from negative to positive also more or less halving the difference. For the most inner point 19 the reduced time steps show a mean value even higher than in the measurements but very near to it. For this location the difference in the amplitudes of the oscillation is most obvious.

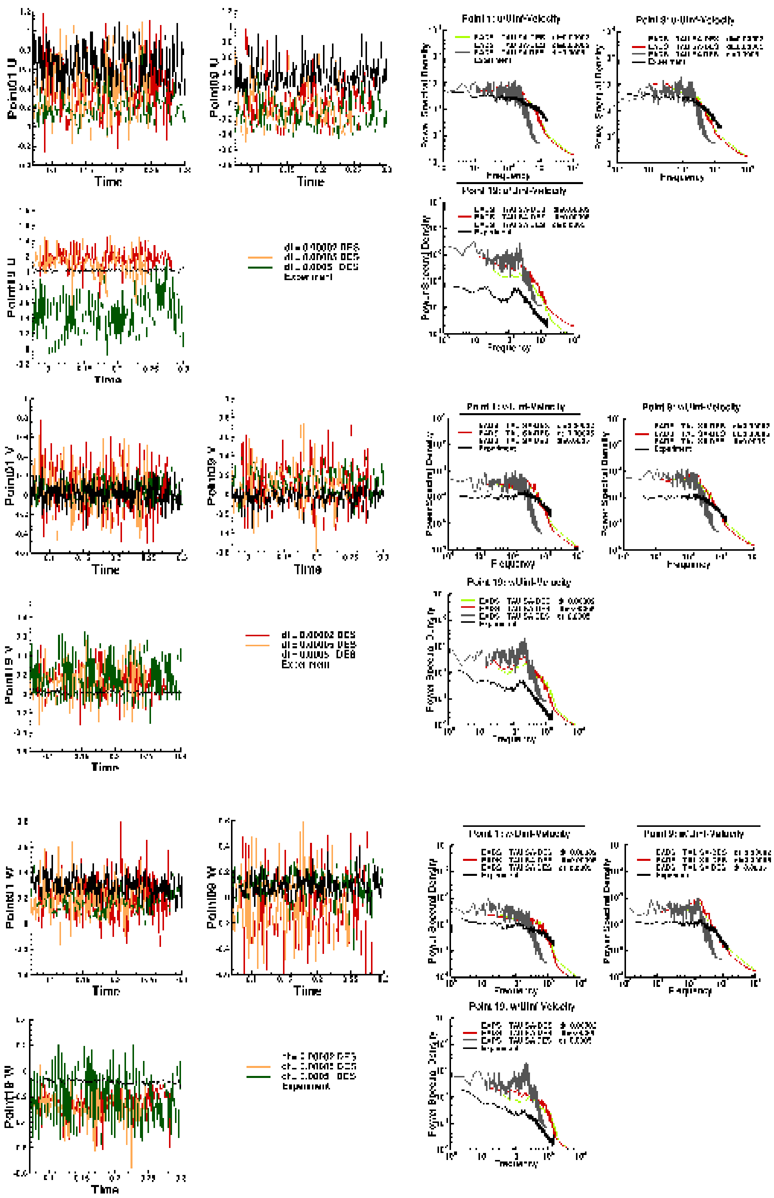

Figure 14: Time history and spectral analysis of velocity components at point 1, 9 and 19

The spectral analysis showing the power spectral density distribution gives better agreement for the high frequencies in correlation with the smaller Δt. Also visible is the higher level of the computational results compared to the experiment as a consequence of the larger amplitudes of the oscillations. This is again most obvious for point 19. For reliable levels at very low frequencies the monitored time gap is too small at the moment for the reduced time step examples. In the experiment dominant frequencies can only be found at point 19 at 200 Hz for all three velocity components and additional at 20Hz for u. These peaks are also represented by the simulations although at 20 Hz for the u-velocity the result suffers from the short monitoring time.

Similar conclusions can be drawn for the two other components. The too high amplitudes in the time history result in too high levels of the PSD value. Better agreement at higher frequencies is visible because of the refined time step size. One must be careful because for example the mean v value at point 19 seems to get worse with the time step reduction. On the other hand, looking at the slice distribution it is recognised that the region of minimum v is located on the wrong side of this point for $\Delta t=5.x10^{-4}$.

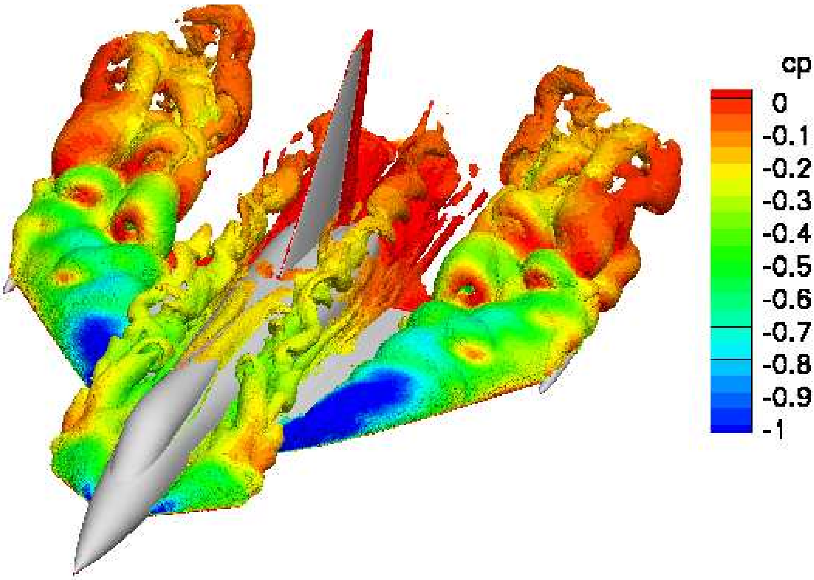

Figure 15: Iso-vorticity surface coloured with cp

The figure above shows the 3D vortex structures coloured with the local cp value. Visible is a complex structure with lots of small vortices. Beneath the main wing vortex many vortex lines flow along the fuselage side wall coming from the canard and the corners. At this inlet angle of attack they start to shift to the centre plane and reaching the height of the vertical fin. This effect causes heavy unsteady structural loads, which may cause structural life cycle problems in a design.

Conclusion

Detached eddy simulations have been carried out for a cavity and a generic fighter.

For the M219 cavity at M=0.85 the SA-DES and the XLES model are applied and show comparable results and good agreement with experiments with regard to the predicted pressure oscillations and main flow features. While the Prms distribution along the bottom wall is in good agreement until x/L=0.6 the offset is slightly increasing towards the end. A similar tendency can be observed at the higher Mach number between x/L=0.5 and 0.8. Apart from a possibly excessive time step used in the calculations, this effect may be caused by a too diffusive free mixing layer leading to a small damping of the calculated pressure fluctuations close to the rear cavity wall. Especially the so called dominant Rossiter frequencies (namely, the 2nd and 3rd mode) representing the acoustic resonance are in very good agreement with the measurements, although the according levels particularly for the SA-DES model are somewhat

overestimated. This has been caused by the relatively large time step used. The underestimation of the 4^{th} tonal mode is also a consequence of the no proper time step size. For M=1.35 the results compares well.
With the generic FA5-5 fighter a realistic industrial configuration was used for a detailed study of the influence of time step reduction upon the SA-DES and SA-DDES model applied. This study was forced by former results generated within the EU project DESIDER which raised the question whether the differences between the turbulence models used, hybrid RANS LES (DES, DDES) and the RANS SST-SAS, are mainly due to the different model approaches or due to the different Δt used.
The comparisons with the experiments performed at the TU Munich shows improving agreement with decreasing time step size although the simulation is not able to present all flow features of the measurements. Compared with former URANS simulations a better correlation with the experimental data base was found with regard to the mean velocity distributions in several slices presented. For the u-component the region indicating negative values vanish almost completely and the qualitative agreement is also improved. Vortex burst found in the experiment to occur at about 60% of the chord is found for the lowest time step at about 64% of cord detected by a small region of negative u-sign.
It is astonishing that the reduction of the time step turns out to have no similar effect with the DDES model. Compared to the time step $\Delta t=1.x10^{-4}$ used by the DLR (Lüdeke 2008) during the DESIDER program no significant differences can be observed. Restarting from a settled DES solution with $\Delta t=2x10^{-5}$ the simulation moved towards the old DLR result showing finally comparable negative u-velocity levels as the DES simulation with $\Delta t=5x10^{-4}$. This behaviour is not understood at the moment and needs further investigation.
It must be stated that the velocity fluctuations are still too high in the monitored points at x/C=0.8 while the mean values are considerable improved. The power spectral density (PSD) for the velocity oscillations is calculated. The distribution also represents the too high amplitudes of the fluctuation. As expected, improvements are generated for higher frequencies by the time step reduction. For reliable levels at low frequencies the monitored time slice is still too small. At least the only dominant frequency at point 19 at 200 Hz is also reproduced by the simulations.
It has been shown that hybrid RANS LES methods are able to simulate the dynamic content of the unsteady flow for the free mixing layers in the cavity case combined with tonal resonance with sufficient accuracy. For the complex unsteady vortex structures around a complete aircraft at high angle of attack, the unsteady content of the flow is still overestimated. The latter result also raises the question about the different sensitiveness between DES and DDES with regard to time step resolution.

References

ANSYS Inc., 2007, "ANSYS CFX, Release 11.0 - Solver Theory Guide, Solver Modelling Guide."

Breitsamter C. (1997): Turbulente Strömungsstrukturen an Flugzeug
konfigurationen mit Vorderkantenwirbeln. PhD thesis, Munich

Gurr, A. et al.: Detached-eddy simulation of a delta wing of a generic aircraft configuration. In: New Results in Numerical and Experimental Fluid Mechanics V. Notes on Numerical Fluid Mechanics and Multidisciplinary Design, vol. 92, pp 463-470. Springer, Heidelberg 2006

W. Haase, M. Braza, A. Revell (Eds.).
DESIDER - A European Effort on Hybrid RANS-LES Modelling.
Notes on Numerical Fluid Mechanics and Multidisciplinary Design,Vol. 103, Springer Verlag (2009).

Kok, J.C., et al.: Extra-large eddy simulation of massively separated flows. In: 42nd AIAA Aerospace Sciences Meeting, AIAA paper 2004-264, Reno, NV, January 5-8, 2004

Lüdeke H., S. Leicher: Unsteady CFD Analysis of a Delta Wing Fighter Configuration by Delayed Detached Eddy Simulation. Advances in Hybrid RANS-LES Modelling, NNFM 97, pp202-211, 2008

Menter, F. R., Egorov, Y. (2005a) Revisiting the turbulent scale equation, In: Heinemann, H.-J. (ed.), Proc. IUTAM Symposium "One hundred years of boundary layer research", Göttingen, Germany, 12-14 August, 2004, Springer-Verlag, 2005.

Menter, F. R., Egorov, Y. (2005b), "A Scale-Adaptive Simulation Model using Two-Equation Models," *AIAA Paper*, AIAA 2005-1095

Rieger H. (2005): First Experiments with Detached-Eddy Simulations in the Aeronautics Industry. Symposium on Hybrid RANS-LES methods, Stockholm, Schweden, 14-15, July 2005

Roshko, A. (1955): Some measurements of flows in a rectangular cutout. NACA TN 3488.

Rossiter, J. E. (1964): Wind tunnel experiments on the flow over rectangular cavities at subsonic and transonic speeds. Rep. Mem. 3438, Aeronautical Research Council.

Spalart, P. R., Jou, W.-H., Strelets, M. and Allmaras, S. R. (1997): Comments on the feasibility of LES for wings and on a hybrid RANS/LES approach. In Advances in DNS/LES: Proceedings of the First AFOSR International Conference on DNS/LES. Ed. Liu, C. and Liu, Z., Greyden Press, Columbus.

Spalart, P.r., Deck, S., Shur, M.L. et al. (2006): A new Version of Detached-Eddy Simulation, Resistant to Ambiguous Grid Densities. Theoretical and Computational Fluid Dynamics, Volume 20, Number 3.

Stanek, M. J., Raman, G., Kibens, V., Ross, J. A., Odedra, J. and Peto, J. W. (2000): Control of cavity resonance through very high frequency forcing. AIAA Paper 2000-1905.

Schwamborn, D., Kroll, N., Heinrich, R. (2006): The DLR TAU-code: recent Applications in Research and Industry. European Conference on Computational Fluid Dynamics, Egmond ann Zee, ECCOMAS CFD 2006